Eur. Phys. J. B **46**, 177–186 (2005)
DOI: 10.1140/epjb/e2005-00225-1

THE EUROPEAN PHYSICAL JOURNAL B

Current dependent reorganization in superconducting $Y_1Ba_2Cu_3O_{7-\delta}$

A. Kiliç[a], K. Kiliç, H. Yetiş, and O. Çetin

Abant Izzet Baysal University, Department of Physics, Turgut Gulez Research Laboratory 14280 Bolu, Turkey

Received 4 March 2005
Published online 19 July 2005 –

Abstract. We present strong non-linear dynamic responses developing due to magnitude and type of driving current in bulk polycrystalline superconducting $Y_1Ba_2Cu_3O_{7-\delta}$ sample at zero magnetic field. Several novel types of dynamic changes induced by the transport current were observed via the time evolution of the voltage ($V-t$ curves). The physical observations appearing in $V-t$ curves were interpreted mainly with the reorganization of driving current in a multiply connected network of weak-link structure. It was found that such a dynamic process could cause an enhancement or suppression in superconducting order parameter due to the magnitude of the driving current and coupling strength of weak link structure together with the chemical and anisotropic states of the sample. It was shown that the general behavior of decays evolving in $V-t$ curves is consistent with an exponential relation which is analogous to the glassy state relaxation.

PACS. 74.72.Bk Y-based cuprates – 74.25.Qt Vortex lattices, flux pinning, flux creep

Introduction

The description of the flux motion in high temperature superconductors (HTSC) is quite interesting and still a complicated problem. A common property of HTSC is the observation of the unusual fast relaxation in magnetization measurements. This behavior has been mainly interpreted in terms of the large giant flux creep effect [1]. However, some magnetic properties of HTSC are far from the description of the conventional flux creep theory and are interpreted in terms of the field/current induced glassy effect rather than the usual theories. Such an effect reminding the spin glasses was first reported by Müller et al. [2] and, then, reported in a bulk superconducting $Y_1Ba_2Cu_3O_{7-\delta}$ (YBCO) sample by Karimov and Kikin too [3]. The experimental results involving the glassy state relaxation given in these studies could be explained by considering the hierarchy of energy barriers together with the existence of a large number of energy states. Within this description, it is assumed that the difference in the energy between the neighboring barriers are small, while the difference between the more distant barriers is higher. Due to the external force or the thermal activation, the vortices can overcome easily the neighboring barriers, but fall in a deeper barrier. Such an energy landscape associated with the *frustrated* superconducting domains coupled by weak links directly leads to the concept of the superconducting glass model. Furthermore, this model also gives reasonable results about the decay of voltage of both zero field cooled and field cooled sample below T_c [3]. We note that the theoretical models [4] and numerical simulations [5,6] reproduce mainly the equilibrium and non-equilibrium properties of the superconducting glass state. It is argued that the superconducting glass state is originated from the short coherence length of HTSCs, which favors, in particular, the formation of the disordered weak link network in polycrystalline samples [7–9].

The recent transport measurements [10–16] on the dynamics of the vortices in Type-II superconductors show many interesting and unusual results, such as history dependent time effects [10], strong metastability [12], slow voltage oscillations including memory effects [13], etc. Henderson et al. [12] showed that high vortex mobility could be obtained for the alternating bidirectional currents and no apparent vortex motion for dc and unidirectional currents in a single crystalline sample of 2H-$NbSe_2$. Xiao et al. [11] reported quite interesting results in Fe-doped single crystalline of 2H-$NbSe_2$ by using the fast transport measurements that the current reorganizes the vortices into new states and a long lived memory effect develops during this process. Another unusual result was observed in de-twinned single crystalline of $Y_1Ba_2Cu_3O_{7-\delta}$ (YBCO) sample by Gordeev et al. [13]. These authors provided an evidence of slow voltage oscillations due to asymmetric bidirectional currents. A generic model which accounts for these observations has been proposed by Paltiel et al. [14] by considering the experimental studies on a single crystalline sample of 2H-$NbSe_2$.

On the other hand, the experiments concerning the transport relaxation on polycrystalline bulk

[a] e-mail: kilic_a@ibu.edu.tr

$Y_1Ba_2Cu_3O_{7-\delta}$ sample have revealed that there is a considerable dynamic process in transport measurements to be taken into account [15–17]. It was shown by Kiliç et al. [16,17] that the generic model proposed by Paltiel et al. [14] could be also applied for polycrystalline YBCO samples. Another interesting phenomena associated with the vortex dynamics is the direct observation of non-stationary flux patterns and current distributions by using of the magneto-optical imaging method, which lead to the significant time effects related to the relaxation phenomenon as a function of both amplitude of current and duration time [18]. The earlier studies showed that the inductive method used by many authors provides a powerful instrument to monitor the field dependent reorganization in investigation of the Type-II superconductors [19–23]. van de Klundert et al. [20] and Gijsbertse et al. [21] studied the response of a slab subject to alternating fields of trapezoidal waveform (single or double) and explored the major mechanisms contributing to the dissipation process. It was shown that the experimental results are consistent with the conventional diffusion theory solved analytically for a slab geometry under the relevant conditions [20,21,24].

The aim of the present study is to investigate the influences of continuous dc current, and unidirectional and bidirectional driving currents having different waiting times on the time evolution of voltage $[V(t)]$ in polycrystalline superconducting $Y_1Ba_2Cu_3O_{7-\delta}$ (YBCO) material at zero field, in detail. We present the experimental observations on the transport relaxation measurements, so called $V-t$ curves, as a function of driving current, I, and temperature, T, for bulk polycrystalline superconducting YBCO material at zero field. We find that a relative increase in dissipation is observed for bi-directional currents as compared to that of continuous ones. It was observed that the response becomes zero as the unidirectional or continuous current is interrupted, while, the reduction in current to a finite value results in a decay in response rather than an abrupt drop to zero. On the other hand, the decays, or the decays together with transition resulting in superconducting or nonsuperconducting state were also observed on both short and long time scales. Furthermore, it was shown that the decays are consistent with an exponential relation which is analogous to the glassy state relaxation in a multiply connected network of the weak-link structure. We interpreted the physical observations appearing in $V-t$ curves mainly in terms of suppression or enhancement of local superconducting order parameter by the transport current (or associated vortices). In addition, the diffusion of the transport current in a resistive medium was considered as a possible alternative description of the $V-t$ curves.

Experiment

The YBCO sample was prepared from the high purity powder of Y_2O_3, $BaCO_3$ and CuO by using the conventional solid state reaction. In order not to apply high currents and to reduce the possible heating effect which will occur at current leads, the sample for the transport measurements was shaped carefully in the dimensions of length $l \sim 4$ mm, width $w \sim 0.1$ mm, thickness $t \sim 0.2$ mm. After the shaping of the sample, the four conductive pads were placed onto the sample by using silver paint and annealed ∼1–2 hours at 150 °C under O_2 atmosphere. The pure copper wires were attached by silver paint. The measured contact resistance by using the three point method was of order of $\sim 10^{-3}\ \Omega$ below T_c and $\sim 10^{-2}\ \Omega$ at room temperature. In this case, the power dissipated at the current contacts would be $\sim 6.5 \times 10^{-6}$ watt for a current of $I = 80$ mA, and, of course, this would have no dramatic effects on the evolution of the $V-t$ curves. The transport measurements were carried out using standard four-point method, and performed in a closed cycle He-refrigerator (Oxford Instruments (OI) CCC1104). In the experiments, Keithley-182 with a resolution 1 nV and Keithley-220 were used in measuring the sample voltage and applying the current, respectively. The temperature was recorded by a calibrated 27 Ohm Rhodium-Iron thermocouple (OI Calibration number 31202), and a temperature stability better than 10 mK was maintained during the experiments (OI, ITC-503 temperature controller) [15–17]. Further, in the measurements, ITC-503 is programmed and the sample is cooled down from room temperature to 120 K with a rate of ∼3 K/min, and, then, a slower cooling rate of ∼1 K/min is preferred.

In this study, the time evolution of voltage ($V-t$ curves) was measured for continuous dc current, and unidirectional and bidirectional driving currents having different waiting times (WT). We note that, for our purpose, the commercial current source Keithley-220 and Keithley-182 are fairly relevant to form such type of currents and to read low voltage levels with a large precision, respectively. The measured voltage is the average value of 5 readings for each data point. After the current is applied, just at this time, we start to measure the developing voltage across the sample as a function of time. Thus, monitoring of all details of the time evolution including the transient effects becomes available. In the experiment, to create a quenched state, the dc current was interrupted or reduced to a finite value.

The YBCO sample whose results are presented in this paper has zero resistance at ∼92 K with a transition ΔT_c of about 3 K at zero field and zero field critical current density of ∼25 A/ cm^2 at $T = 88$ K by using the 1 μV/cm criterion.

Experimental results

Figure 1a shows the time evolution of the voltage $V(t)$ (i.e., $V-t$ curves) for continuous dc currents of +30 and –30 mA, separately, at $T = 88$ K. As can be seen, the $V-t$ curves evolve in three-stages: in first stage, initially, any measurable voltage response is not observed within a certain delay time of ∼10 s. In second stage, the absolute response starts growing up non-linearly for both current values (in absolute value of V). Finally, in third stage, after ∼40 s, the voltage in both curves reaches nearly a

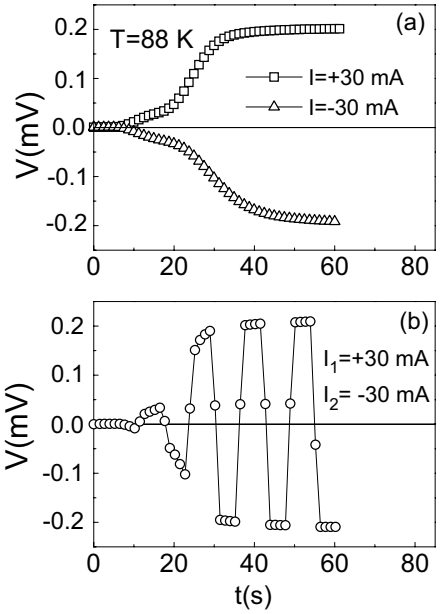

Fig. 1. (a) The time evolution of the voltage the $V-t$ curve at constant continuous dc current of $I = \pm 30$ mA at 88 K. (b) The effect of bidirectional current which is switched periodically forth and back between –30 and +30 mA on the evolution of the $V - t$ curves. The waiting time is 6 s.

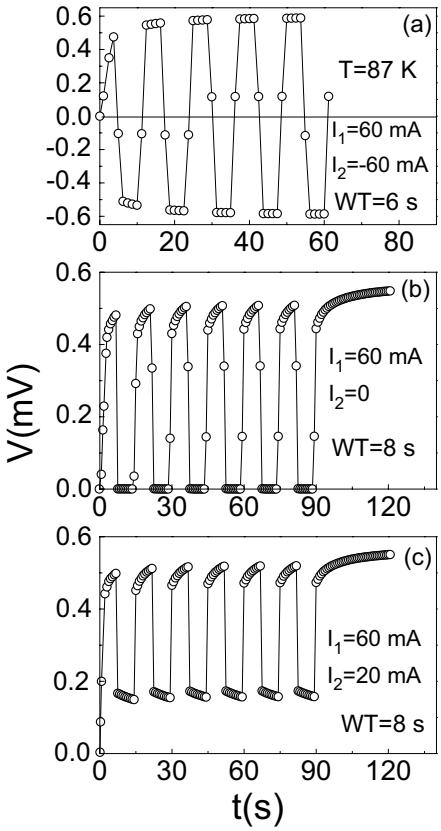

Fig. 2. (a) The effect of bidirectional current with the amplitude of ±60 mA and waiting time of 6 s on the $V - t$ curve at $T = 87$ K. (b) The effect of unidirectional current with the amplitude of 60 mA on the evolution of the $V - t$ curves. The current is switched periodically from $I_1 = 60$ mA to zero value with waiting time of 8 s. Note that the continuous current is left at $I_1 = 60$ mA for $t > 90$ s. (c) The effect of the reducing of unidirectional current periodically from $I_1 = 60$ mA to a finite value of $I_2 = 20$ mA with a waiting time of 8 s on the $V - t$ curve. Here too, the continuous current of 60 mA is left on the sample for $t > 90$ s.

steady state. On the other hand, a current was applied in forward direction for a while (i.e., for a certain waiting time WT) and, then, it was applied in reverse direction during the same the waiting time. This process was repeated periodically several times, and, thus, repetitive regular current cycles were obtained as a function of time (i.e., bidirectional current). Figure 1b and c illustrate the time evolution of the voltage for such a bidirectional current which is switched periodically forth and back between –30 and +30 mA with a waiting time (WT) of 6 s. Here too, after a certain delay time, a non-linear increase in sample voltage develops with time. It is also seen that the voltage jumps up very rapidly to larger values for each subsequent reversal as the direction of the current is reversed. For the waiting time of 6 s, the response becomes nearly saturated after ∼30 s.

Figure 2a shows the time evolution of the voltage for a bidirectional current which is switched forth and back between –60 and +60 mA with a waiting time (WT) of 6 s for several repetitive cycles at $T = 87$ K. Within a very short time interval, a rapid increase in voltage is observed, then, a nearly steady state is established inside the sample as in Figure 1b. Figure 2b shows a $V - t$ curve measured for $I_1 = 60$ mA, $I_2 = 0$ with a waiting time of 8 s. As is seen from the figure, the voltage drops very rapidly to the zero value as the driving current is switched to zero, and, when the current is restored again within WT = 8 s, the voltage increases rapidly, and, then, approaches nearly to its previous value where the current is switched to zero. After several repetitive cycles, at $t > 90$ s, the driving current was switched to $I_1 = 60$ mA and it was left on the sample. We note that a similar observation has been reported in single crystalline sample of 2H-$NbSe_2$ by using the fast transport measurements by Xiao et al. [11]: One of the interesting observations in their study is that, as in our case, the sample voltage drops instantaneously zero value, as the driving current was interrupted.

In order to investigate further the influence of periodic driving current on the evolution of the $V - t$ curves, during the measurements, a current switched periodically between two different current values, I_1 and I_2, at the same direction (i.e., unidirectional driving current) was applied on the sample, differently from the study of Xiao et al. [11]. Figure 2c shows such an experiment which the current is reduced periodically from $I_1 = 60$ mA to $I_2 = 20$ mA with WT of 8 s. After several repetitive cycles, the dc current of $I_1 = 60$ mA was left on the sample for $t > 90$ s. Here, differently from Figure 2b, whenever the driving current is reduced to 20 mA, the voltage drops instantaneously to a finite value and decays during WT of 8 s. It will be shown later that the decay in V is fairly non-linear and depends

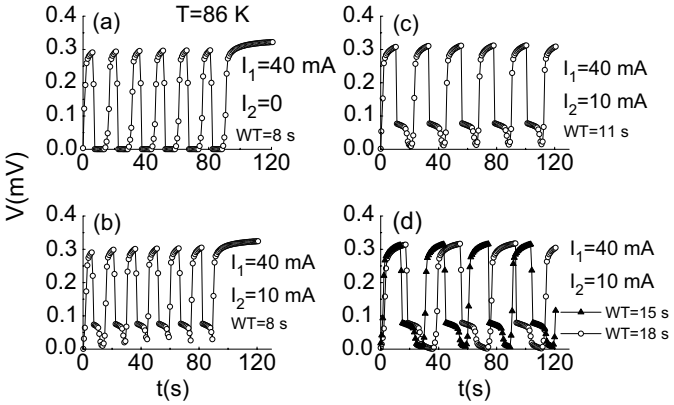

Fig. 3. The effect of the waiting time on the $V-t$ curves at 86 K as the current is periodically and unidirectionally reduced from I_1 to a finite value of I_2 for different waiting times (WT). (a) I_1= 40 mA and I_2 = 0. WT = 8 s. (b) I_1= 40 mA and I_2 = 10 mA, WT = 8 s. (c) I_1= 40 mA and I_2 = 10 mA, WT = 11 s. (d) I_1= 40 mA and I_2 = 10 mA, WTs = 15 and 18 s.

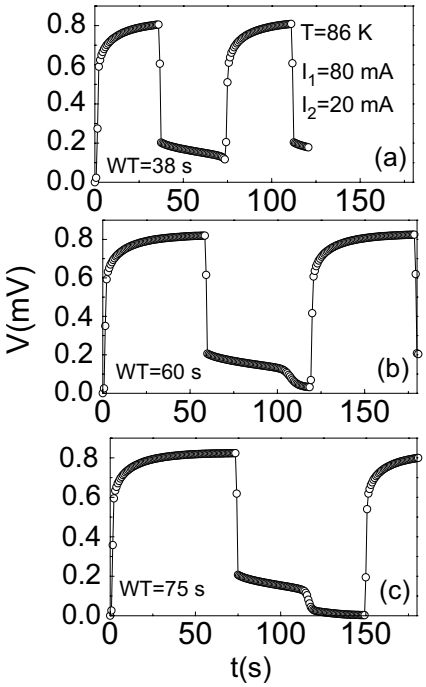

Fig. 4. The evolution of $V-t$ curves whose the current is switched periodically from $I_1 = 80$ mA to $I_2 = 20$ mA at $T =$ 86 K for different waiting times of (a) WT = 38 s, (b) WT = 60 s, and (c) WT = 75 s. Note that the superconducting state develops as the waiting time increases.

strongly on the magnitude of the current value of I_1, I_2, and also the value of WT.

Figures 3a–d illustrate mainly the time evolution of the voltage for unidirectional periodic currents with different waiting times at $T = 86$ K. Figure 3a shows a $V-t$ curve measured under the repetitive regular current cycles for $I_1 = 40$ mA, $I_2 = 0$ with WT = 8 s. As is seen from Figure 3a, when the current is interrupted, the sample voltage becomes abruptly zero, whereas a non-linear increase in voltage grows up as the current is again switched to $I_1 = 40$ mA after WT = 8 s and the voltage response tends to be nearly saturated with time when the dc current of 40 mA was left on the sample. In Figures 3b–d involving different WT of 8, 11, 15, and 18 s, this time, the driving current was reduced from $I_1 = 40$ mA to a finite value of $I_2 = 10$ mA, rather than removed completely. Differently from Figure 3a, whenever the driving current is reduced to 10 mA, the voltage response drops instantaneously to a finite value (not zero) and decays for a while and undergoes a smooth transition tending to become zero provided that the waiting time is long enough as in Figure 3d.

Figures 4a–c show the effect of waiting time on the evolution of the $V-t$ curves for $I_1 = 80$ and $I_2 = 20$ mA at 86 K. Note that I_1 and I_2 are doubled with respect to the $V-t$ data given in Figures 3b–d. The common feature of all these $V-t$ curves is that the voltage increases nonlinearly before entering into nearly a steady state for $I_1 = 80$ mA, and, then, in the second stage where the current is reduced to 20 mA, the voltage decays. As the waiting time increases, the decay in sample voltage results in a superconducting state after a non-linear transition. The time dependence of response shows that the waiting time must be long enough to observe the evolution of superconducting state. Doubling of I_1 and I_2 with respect to Figure 3d causes a considerable delay in monitoring of the transition to the superconducting state. For instance, the onset time of such transition increases by a factor of ∼4 with respect to the $V-t$ data given in Figure 3d. Thus, it can be suggested that the evolution of the $V-t$ curves not only depends on waiting time but also depends on the magnitude of I_1 and I_2. In what follows, those effects are investigated in more detail.

To further examine the effect of the magnitude of the driving current on the $V-t$ curve, this time, a dc driving current of $I_1 = 80$ mA was applied for the time of ∼40 s. Then, the current was reduced from I_1 to a finite value of I_2, and it was left on the sample up to ∼300 s. Figure 5 shows such typical $V-t$ curves measured at $T = 86.5$ K for different current values of $I_2 = 23$, 25, 27, 28 and 30 mA, respectively. In all $V-t$ curves, the voltage decays over time after reducing of the current to I_2. On the other hand, note that the decay in voltage for $I_2 = 23$ mA continues for a whereas and, then, shows a smooth transition to the superconducting state, while, in the $V-t$ curve for $I_2 = 25$ mA, although a transition evolving to the superconducting state is observed, the zero resistance state is not satisfied for this current value yet. Another interesting case in this figure is the behavior of the $V-t$ curve where the current I_2 is 27 mA: The voltage in this $V-t$ curve decays over time as in the other curves, and, then, it shows a wide transition, as if, to reach the superconducting state. As the time progresses, however, it passes a minimum at around ∼128 s and begins to increase over time approaching to the voltage response of the $V-t$ curve measured for $I_2 = 28$ mA. On the other hand, the $V-t$ curves measured

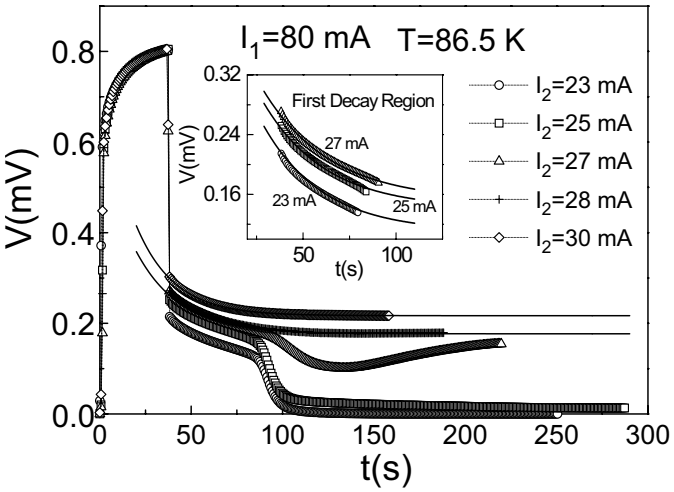

Fig. 5. Time evolution of the $V-t$ curves at $T = 86.5$ K as a function of I_2 with $I_1 = 80$ mA, where $I_2 = 23$, 25, 27, 28, and 30 mA. After the current of I_1 is applied for the waiting time of 40 s, it is reduced to I_2 and left on the sample. The inset illustrates the first decay region up to the transition for $I_2 = 23$, 25, and 27 mA, in detail. The solid lines in both main panel and inset are the calculated curves by using equation (1).

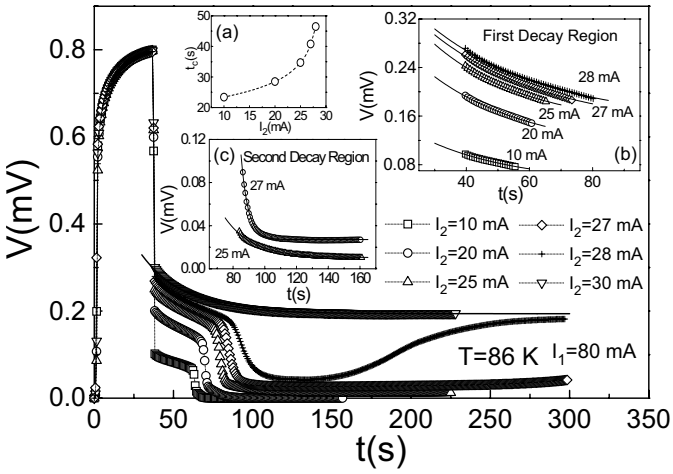

Fig. 6. Time evolution of the $V-t$ curves at $T = 86$ K as a function of I_2 with $I_1 = 80$ mA, where $I_2 = 10$, 20, 25, 27, 28 and 30 mA. The inset 'a' represents the variation of critical time t_c with I_2. Here, the t_c is the elapsed time from the beginning of the voltage decay to the onset of the transition time for the first decay region. The inset 'b' represents the first voltage decays corresponding to the time interval of $40-80$ s before the transition. The inset 'c' shows the second decays corresponding to the time interval of $85-165$ s after the transition. The solid lines in the main panel and in the insets show the best fits of equation (1).

for $I_2 = 28$ and 30 mA show only a remarkable smooth decay over time without undergoing any transition.

To observe the effect of the temperature on the evolution of the $V-t$ curves, we carried out similar measurements at 86 K applying the same experimental procedure described in Figure 5. The reason of choosing a temperature point which is close to that of Figure 5 is that the evolution of $V-t$ curves are very sensitive to the temperature change. The measurements were repeated for the selected current values of $I_2 = 10$, 20, 25, 27, 28 and 30 mA, respectively. Figure 6 which contains these $V-t$ curves exhibit similar interesting properties as in Figure 5: When the magnitude of current is reduced from $I_1 = 80$ mA to I_2, the sample voltage drops abruptly, and, then, it decays nonlinearly up to a certain time value t_c (critical time) which depends on the magnitude of I_2. This dependence is depicted in the inset 'a' and it is seen that there is a non-linear relation between t_c and I_2. For $t > t_c$, this time, a smooth transition appears in a relatively narrow time region, except $I_2 = 30$ mA. It should be noted that the width of transition increases with increasing of I_2. We also observed that the decays for $I_2 = 10$ and 20 mA result in a transition to superconducting state (since V goes to zero), while the voltage for $I_2 = 25$ and 27 mA continues to decrease gradually over time together with the transition and more interestingly, after $t \sim 200$ s, the voltage for $I_2 = 27$ mA tends to increase with time after a wide transition. On the other hand, the $V-t$ curve seen at $I_2 = 28$ mA in Figure 6 illustrates a different behavior from the $V-t$ curve seen at the same current value of I_2 in Figure 5. In Figure 6, at this current value, after $\sim$135 s, the voltage begins to increase non-linearly over time and approaches asymphtotically to the voltage response of $I_2 = 30$ mA. Finally, it is seen that the behavior

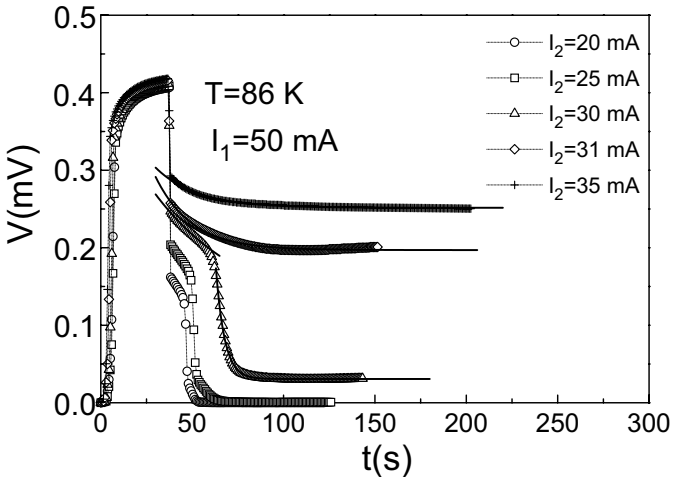

Fig. 7. Time evolution of the $V-t$ curves at $T = 86$ K as a function of I_2 with $I_1 = 50$ mA, where $I_2 = 20$, 25, 30, 31, and 35 mA. The solid lines are the calculated curves by using equation (1).

of $V-t$ curve at $I_2 = 30$ mA does not change as compared to that of Figure 5.

Figure 7 depicts the evolution of the $V-t$ curves measured for $I_1 = 50$ mA and $I_2 = 20$, 25, 30, 31 and 35 mA at $T = 86$ K. Here, it is possible to observe how the decreasing of the magnitude of the current I_1 affects the behavior of the $V-t$ curves. First, it is observed that the transition to superconducting state after the non-linear decrease in voltage is sharper for the low current values of $I_2 = 20$

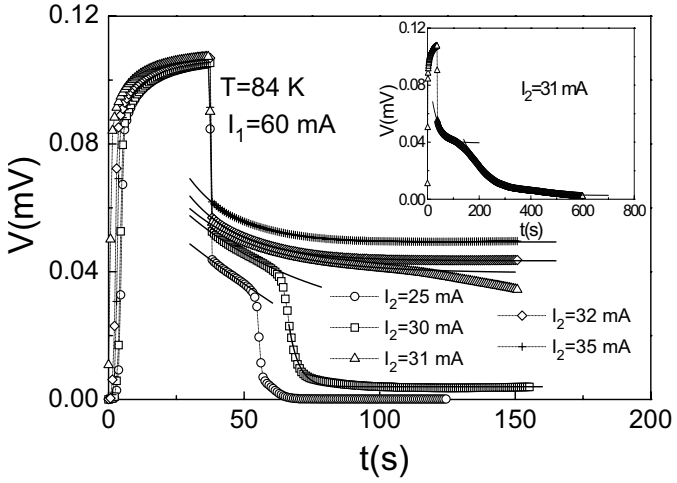

Fig. 8. Time evolution of the $V-t$ curves at $T = 84$ K as a function of I_2 with $I_1 = 60$ mA, where $I_2 = 25$, 30, 31, 32, and 35 mA. Inset shows the long time evolution of the $V-t$ curve of $I_2 = 31$ mA. The solid lines in both main panel and inset are the calculated curves by using equation (1).

and 25 mA as compared to that of the observed for the same current values in Figure 6. Second, the required time to observe the onset of the transition to superconducting state becomes shorter. For instance, the onset time of the transition which corresponds to $I_1 = 50$ and $I_2 = 20$ mA appears at ∼50 s in Figure 7, whereas this value is ∼75 s at $I_1 = 80$ mA for the same I_2 value in Figure 6. Finally, a smooth decay in voltage is observed without transition at the currents of $I_2 > 30$ mA.

In order to give a further support for the physical case appearing in the $V-t$ curves presented in Figures 4–7, similar $V-t$ measurements were repeated at a different temperature point. Figure 8 shows the $V-t$ curves taken at 84 K for $I_1 = 60$ mA and $I_2 = 25$, 30, 31, 32 and 35 mA. As is seen from the main panel, reducing of I_1 from 60 mA to a lower values of I_2 reveals similar time effects presented in Figures 4–7. The transition to superconducting state is observed for $I_2 = 25$ mA, while, the transition observed for $I_2 = 30$ mA does not result in a superconducting state yet. An interesting case is seen for the current value of $I_2 = 31$ mA: In this $V-t$ curve, the voltage decays smoothly for a while and makes a wide transition tending to reach the superconducting state. In the inset of the main panel, the details of the time evolution of the voltage response associated with $I_2 = 31$ mA are given in an extended time interval of $0-600$ s. As is seen, to reach the superconducting state will take a considerable time more than 10 min. On the other hand, for the other current values of $I_2 = 32$ and 35 mA, only a smooth decay in voltage is observed.

Discussion

We now concentrate on the data given in Figure 1 and Figure 2. In Figure 1a, there is a process with three-stage. In the first stage, we suggest that the transport current (or associated vortices injected from the surface of the sample) tries to distribute itself for a while by penetrating through the weak link network which is operating fully. In this stage, no measurable voltage can be considered as an indication of that the weak link network are not destroyed much by the current which meanders along the nonresistive flow channels (regions). The initial delay appearing in $V-t$ curves can be attributed to that the superconducting order parameter maintains its prior spatial configuration while the driving current organizes itself inside the sample. As the time progresses, the current will begin to threaten the weak links and will cause a dissipation. In this second stage, due to the gradual penetration of the current, when the first link is broken, the current density will increase automatically in the neighboring area inside the sample and will try to disrupt other weak links due to its magnitude. Thus, an enhancement in dissipation together with a dynamic process triggered by the current will appear. The nonlinear increase in voltage seen in this stage can be evaluated as an indication of the coexistence of the disruption and reconstruction of the weak link structure. However, the voltage response shows that the competition between two physical mechanisms develops mostly in favor of disruption in time. Finally, at last stage, a steady process is established within the time scale of the experiment, since the transport current nearly completes the redistribution process, depending on its magnitude. The process with three-stage is also observed in Figure 1b and in Figure 2a, although the current is driven periodically forth and back for a given time interval.

It can be suggested that Joule heating [25,26] at current contacts or local heating effects in microscopic scale [25–27] (i.e., hot spot effect) contributes to the measured dissipation. First, as the power dissipation of ∼6.5 μW at contact area is considered, Joule heating effect should have a negligible contribution to the measured dissipation, and, therefore, would cause no dramatic effect on the evolution of the $V-t$ curves. However, it is worth nothing to discuss the hot-spot effect as a small scaled heating source. During the evolution of the $V-t$ curves, the internal energy of the superconductor may increase in time since the transport current is left on the sample for a while. By considering that the transport current exceeds a critical value, i.e., Josephson critical current corresponding to the junction network, Josephson coupling strength between the grains can be reduced considerably and the weak links can be successively switched off by increasing the number of the decoupled grains. This implies that more current into the neighboring channels is brought as the time progresses. On the other hand, the weak links and the regions where the weak superconductivity exits will start a gradual transition to normal state and become more resistive by enhancing the power dissipation. Such a process can trigger the formation of new resistive regions and thus can cause again to increase the power dissipation, and so on. We note that the power dissipation can reflect itself as releasing of small scaled heat along the resistive regions and can extend over the whole sample since

the junction network is highly ramified, not independent of each other. In this way, a contribution arising from the hot-spot effect to the measured voltage can be expected, and, as a result, it can play a role in the increase of the resistance of the sample until the maximum voltage is obtained. As can be seen from Figure 2b and Figure 3a, zero voltage is observed after switching the driving current to zero. In one hand, this case demonstrates that there is no residual current flowing along resistive flow channels to be relaxed; in the other hand, it implies that the weak links which are broken form a coherent state within a very short time and heat transfer along the junction network disappears very rapidly. Therefore, we suggest that the voltage arising from the local heating effects developing inside the sample has a small fraction of the measured voltage, otherwise, there would be an observable time dependent voltage decay in these $V - t$ curves. At this point, we would like to note that such an experiment represented in Figure 2b and Figure 3a can be assumed a way to test whether the time effects appearing in $V - t$ curves originate from the heating effects, such as Joule heating at current contacts and hot spot effect, or not. In view of the discussion given above, we conclude that the observation of zero voltage for $I = 0$ rules out the thermal relaxation. On the other hand, the non-linear increase appearing in voltage whenever the current increases to 60 mA in Figure 2b and 40 mA in Figure 3a can be evaluated as a gradual disruption of the weak-links by the driving current.

We now consider the time effects induced by the transport current in Figure 2c, Figures 3b–d, Figures 4a–c, and Figures 5–8. It can be suggested that the time effects appearing in these $V - t$ curves are related to the suppression or enhancement of the superconducting order parameter [28,29]. As is discussed in detail by Dimos et al. [28], and Hilgenkamp and Mannhart [29], the grain boundaries and their intrinsic characteristics are responsible for the low current carrying capacity of polycrystalline HTSC. It is also argued and shown by these authors that the intergranular currents are quite sensitive to the misorientation angle between the adjacent grains. Therefore, the strong field dependence of the intergranular currents is attributed to the suppression of the local order parameter due to the structural features of those grain boundaries. It can be suggested that abruptly reducing the current from I_1 to I_2 causes spatially a quenched state in the distribution of the transport current (or associated vortices) in a multiply connected network of the weak links where the coherent state is destroyed by I_1. In this case, within a very short time, the transport current in the quenched state can re-distribute itself spatially and can dissipate less energy since $I_2 < I_1$. On the other hand, the reduction in the driving current will also stimulate gradually the enhancement in the superconducting order parameter over time, so that this is the reason why we observe a decay in the sample voltage for a while. As time progresses, depending on the magnitude of I_1 and I_2, and also to the structural disorder, chemical and anisotropic states of the sample, the decay can result in a transition to the superconducting state [Fig. 3d, Fig. 4c, and Figs. 5–8]. We correlate the transition seen as a function of I_2 to that most of the weak links begins gradually and coherently to reoperate, and, thus, a full coherent state is satisfied inside the sample after the voltage response becomes zero.

To distinguish two different decay regions observed after the current is reduced to I_2, we classify the decays as: first decay region involving the decay observed in $V - t$ curves up to the transition (the first decay region also includes the voltage decays which do not exhibit any transition), and second decay region involving the voltage decay after the first decay region.

On the other hand, a different behavior in the $V - t$ curves is seen at $I_2 = 27$ mA in Figure 5 and at $I_2 = 28$ mA in Figure 6. The common behavior seen in these $V - t$ curves is that the transition from the first decay region to second one is fairly wide and non-linear, and, then, the voltage begins to increase and approaches asymptothically to that of $I_2 = 28$ and 30 mA, respectively. We suggest that this interesting behavior can be explained in the frame of a generic model recently proposed by Paltiel et al. [14]. Their experimental studies on a single crystalline sample of 2H-$NbSe_2$ have shown that a competition between the injection of a disordered vortex phase at the sample edges and the dynamic annealing of the meta-stable state of the disorder by the transport current plays a key role. In this model, it is argued that the driving current which anneals the meta-stable disorder serves as an effective temperature in the usual sense as in the statistical mechanics. In a recent study, we showed that this generic model could also be applied for the investigation of vortex dynamics in HTSC [16,17]. In our case, the sample edges can be taken as grain boundaries in polycrystalline YBCO sample. We suggest that the gradual nonlinear increase in V over time in the second decay region can be evaluated as a direct evidence of the dynamic annealing effect of the driving current on the weak link structure [16,17]. The data show that the driving current reduces the coupling strength between the weak links by depressing locally the superconducting order parameter and provokes disruption of many of weak links which try to form a coherent state. Thus, within this description, we conclude that the increase in response can be evaluated as a gradual increase in the size of the dissipative non-superconducting channels.

After reducing the current from I_1 to I_2, a direct comparison of the $V - t$ curves given in Figure 6 and Figure 7 shows that the total required time to reach the onset of transition and to satisfy the superconducting state realized for lower current values of I_2 increases with increasing of I_1. For instance, in the $V - t$ curves measured for $I_2 = 20$ mA in Figure 6 and Figure 7, the total required time values to satisfy the superconducting state are $\sim$35 s for $I_1 = 80$ mA and $\sim$15 s for $I_1 = 50$ mA, respectively. We suggest that this phenomena arises from the fact that the superconducting order parameter is suppressed much more at high values of I_1 as compared to that of the lower ones. In another words, the local non-superconducting regions expands relatively at high values of I_1. However, as the current is switched to I_2, the effective size of

dissipative non-superconducting flow channels begins to decrease gradually with time and, thus, to reach the superconducting state takes longer times at higher values of I_1.

It is well known that the the glassy state relaxation (GSR) fits a stretched exponential time dependence of $\sim\exp(-t/t_o)^\alpha$ to describe the time decay in the remanent magnetic moment, where t_o is the characteristic time and the exponent α is a temperature dependent constant [2,3]. We note that, in this expression, the time evolution and degree of ordering of individual magnetic moments can be determined via the exponential term given. In order to create a glassy state as in the spin glasses, one of the requirements is that the transport current or the external magnetic field should be interrupted completely or partly during the measurements. During the course of the experiments, the driving current is abruptly reduced a finite value or interrupted completely. Thus, it becomes possible to create a quenched state which is unstable in time, and the measurable time independent parameters of the system become remarkably time dependent. We now show that the first decay regions appearing in $V-t$ curves are consistent with an empirical exponential expression which is analogous to the glassy state relaxation (GSR) [3]:

$$V(t) - V_o = A\exp(-t/t_o), \qquad (1)$$

where t_o is a characteristic time and A is a coefficient. The solid lines seen in both the main panels and insets in Figures 5–8 represent the best fits of equation (1) to the data points. Note that the fitting procedure considers the first and second decay regions separately. It is seen that, in general, there is a reasonable agreement between the calculated curves and experimental data. For the first decay regions in the $V-t$ curves given in Figure 6, the variation of the characteristic time t_o values deduced from the fitting procedure with respect to the driving current of I_2 is illustrated in Figure 9. On the other hand, the voltage decays corresponding to the current values of $I_2 = 20$ and 25 mA given in Figure 7 could not be compared to equation (1) because of the insufficient number of data points associated with the decays developed within a shorter time interval.

Although, for the second voltage decays after the transition in Figure 5, we could not obtain any reasonable agreement with equation (1), the data corresponding to the second decay regions in Figures 6–8 show an agreement. Therefore, we suggest that abruptly reducing of the current from I_1 to I_2 can cause formation of a kind of glassy state associated with its distribution in a multiply connected random weak link network. In such a case, the driving current can reorganize itself into a new dynamic state where the local superconducting order parameter is enhanced or suppressed despite the fact that the driving current is kept constant. For instance, at the current values of $I_2 = 10$ and 20 mA in Figure 6, nearly disappearance of the sample voltage over time can be evaluated as an enhancement in the superconducting order parameter.

As is discussed above in detail, the superconducting glass model gives a reasonable description of the exponential time decay of the sample voltage, however, we

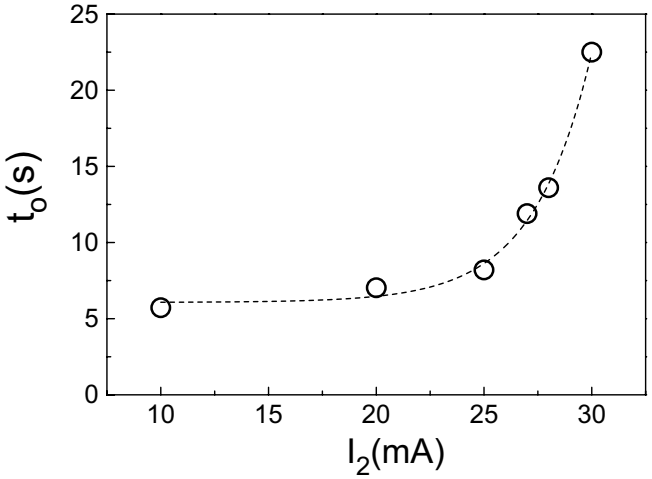

Fig. 9. The variation of the characteristic time t_o values with I_2. t_o is found from fitting of equation (1) to the data points corresponding to the time interval of $40-80$ s before the transition in Figure 6.

note that diffusion of the transport current in a resistive medium can be considered as an alternative possible mechanism. The experimental studies which consider the response of the slab to a steplike variation of the applied field provides an evidence of such a diffusion process [20,21,30]. One of the main observations in these studies is that the induced voltage could exhibit an exponential time dependence due to the magnetic field variation [20,21,30]. Furthermore, the solution of the conventional diffusion equation for a slab geometry under relevant conditions gives a support for the experimental observations and, in particular, confirms the exponential decay of the sample voltage over time [20,21,30]. Within this description, in our case, the external drive can be taken as transport current in place of magnetic field, and, it can be suggested that a conventional diffusion process governs the current dependent reorganization in a multiply connected network of the weak link structure of the polycrystalline YBCO sample. The initial transport current (or associated vortices) penetrates from the outer surface of the sample and meanders along nonresistive flow channels. As the driving current is abruptly reduced to a finite value, at the beginning of the process, a quenched state which is reminiscent of a glassy state can develop. After the quenching, the transport current (or associated vortices) can redistribute itself in a hierarchy of energy landscape, and, thus, as the time progresses, its spatial redistribution which reflects the different degree of order of the penetrated states evolving inside the sample can be expected. Hence, it would be also reasonable to assume that a conventional diffusion model can be considered as an alternative possible mechanism in explaining the time dependence of the voltage, i.e. $V-t$ curves.

Gijsbertse et al. [21] demonstrated that the inductive method enables also to separate the various contributions to the ac losses and has a prominent role in determination

of the various parameters of Type-II superconductors. Therefore, at this point, we suggest that it would be instructive to give a comparison between this technique and our experimental method, which help to understand various properties of the superconducting materials, although they follow different procedures.

The earlier compherensive studies on conventional Type-II superconductors were discussed in terms of the critical state model which enables to distinguish the bulk and surface currents [20,21,23]. One of the best methods in determining the various parameters of the critical state model and also the physical features of Type-II superconductors is the inductive technique, which has many advantages. For instance, the flux and current distributions evolving spatially inside the sample, and flux flow effects could be determined via this method. van de Klundert et al. [20] and Gijsbertse et al. [21], used such a method and studied the inductive response of a superconducting slab (i.e., Nb, and Nb-50%Ti) to an ac magnetic field with trapezoidal time dependence (single or double) and recorded the time evolution of the induced voltage in a pick-up coil around the surface of the sample. For a double trapezoidal waveform, a non-linear increase in the response was observed until the external ac magnetic field is stopped, and, for the constant value of the waveform where the time rate of the applied field takes its highest value, the induced voltage represented an exponential decay in time [21]. Thus, the flux flow properties of the superconducting material under investigation together with the surface screening could be studied. In addition, the recorded voltage in the inductive method is sensitive to the magnitude of the excitation and mimics properly the time variation of the excitation. We note that the induced voltage measured with this technique is a measure of the field dependent motional reorganization.

Our experimental procedure considers the slow transport relaxation measurements and enables to monitor the time evolution of the sample voltage to continuous dc, bidirectional and unidirectional driving currents, respectively, and uses *resistivity* technique. In this way, such slow and fast transport relaxation measurements provide an accurate way to determine the metastable states, motional reorganization, dynamic transitions, and dynamics of driven vortices etc. The slow transport relaxation measurements in the present study reveal that the voltage developing in the direction of the transport current reflects the variation of the driving current in time and gives a measure of the current dependent reorganization evolving inside the superconducting polycrystalline YBCO sample at zero magnetic field.

Finally, we note that, in addition to the other conventional transport and inductive techniques, the measurement technique introduced here is a candidate to be a powerful method to monitor dynamic processes, such as evolution of the reorganization of the transport current (or associated vortices), the transient effects developing in transport measurements, the details of the vortex dynamics and the nature of the vortex state, etc. [16,17].

Conclusion

In this study, novel type dynamical changes generated by the driving current have been observed in a bulk polycrystalline superconducting $Y_1Ba_2Cu_3O_{7-\delta}$ (YBCO) sample via the transport relaxation measurements ($V-t$ curves). The evolution of nonlinear $V-t$ curves was interpreted in terms of the competition between the disruption and reconstruction of the weak links during the spatial organization of the transport current. When the driving current was interrupted, it was observed that the measured voltage is completely zero. This behavior was evaluated that there is no residual current to be relaxed. However, a nonzero voltage decaying with time was recorded when the magnitude of current I_1 is reduced to a finite value of I_2. It was found that, at sufficiently large values of the waiting time, the decrease in voltage could result in a superconducting state, depending on the magnitude of the driving current. It was found for unidirectional and bidirectional currents that the time effects in these measurements strongly depends on the magnitue of I_1, I_2, and the waiting time. We also showed that the decays in voltage over time are consistent with an empirical exponential time dependence, $\sim\exp(-t/t_o)$, which is analogous to the glassy state. In addition, the diffusion of the transport current in a resistive medium was considered as a possible alternative description of the $V-t$ curves. Finally, we conclude that the reorganization of driving current (or associated vortices) in a multiply connected network of weak-link structure could cause an enhancement or suppression in superconducting order parameter due the magnitude of the driving current and coupling strength of weak link structure together with the chemical and anisotropic states of the sample.

This work was supported by TUBITAK/TBAG 2037.

References

1. Y. Yeshurun, A.P. Malozemoff, Phys. Rev. Lett **60**, 2202 (1988)
2. K.A. Müller, M. Takashiga, J.G. Bednorz, Phys. Rev. Lett. **58**, 1143 (1987)
3. Yu.S. Karimov, A.D. Kikin Physica C **169**, 50 (1990)
4. C. Ebner, D. Stroud, Phys. Rev. B **31**, 165 (1985)
5. I. Morgensten, K.A. Müller, J.G. Bednorz, Physica C **153–155**, 59 (1988)
6. I. Morgensten, K.A. Müller, J.G. Bednorz, Z. Phys. B **69**, 33 (1987)
7. G. Deutscher, K.A. Müller, Phys. Rev. B **59**, 1745 (1987)
8. G. Deutscher, Physica C **153–155**, 15 (1988)
9. C. Rossel, Y. Maeno, I. Morgensten, Phys. Rev. Lett. **62**, 681 (1989)
10. W. Henderson, E.Y. Andrei, M.J. Higgins, S. Bhattacharya, Phys. Rev. Lett. **77**, 2077 (1996)
11. Z.L. Xiao, E.Y. Andrei, M.J. Higgins, Phys. Rev. Lett. **83**, 1664 (1999)

12. W. Henderson, E.Y. Andrei, M.J. Higgins, Phys. Rev. Lett. **81**, 2532 (1998)
13. S.N. Gordeev, P.A.J. de Groot, M. Oussena, A.V. Volkozup, S. Pinfold, R. Langan, R. Gagnon, L. Taillefer, Nature **385**, 324 (1997)
14. Y. Paltiel, E. Zeldov, Y.N. Myasoedov, H. Shtrikman, S. Bhattacharya, M.J. Higgins, Z.L. Xiao, P.L. Gammel, D.J. Bishop, Nature **403**, 398 (2000)
15. A. Kiliç, K. Kiliç, O. Çetin, J. Appl. Phys. **93**, 448 (2003); Virtual J. Appl. Supercon. **4**(1), (2003)
16. K. Kiliç, A. Kiliç, H. Yetiş, O. Çetin, Phys. Rev. B **68**, 144513 (2003); Virtual J. Appl. Supercon, **5**(8), (2003)
17. K. Kiliç, A. Kiliç, H. Yetiş, O. Çetin, J. Appl. Phys. **95**, 1924 (2004)
18. A.V. Bobyl, D.V. Shantsev, Y.M. Galperin, T.H. Johansen, M. Baziljevich, S.F. Karmanenko, Supercond. Sci. Technol. **15**, 82 (2002)
19. P. Alais, Y. Simon, Phys. Rev. **158**, 426 (1967)
20. L.J.M. van de Klundert, E.A. Gijsbertse, H.P. van de Braak, Physica B **94**, 41 (1978)
21. E.A. Gijsbertse, M. Caspari, L.J.M. van de Klundert, Cryogenics, **21** 299 (1981)
22. E.A. Gijsbertse, J.L. de Reuver, L.J.M. van de Klundert, Physica B **112**, 24 (1982)
23. H. Vasseur, P. Mathieu, B. Plaçais, Y. Simon, J. Phys.: Condens. Matter **10**, 7193 (1998)
24. T. Kawashima, T. Ezaki, K. Yamafuji, Jpn J. Appl. Phys. **17**, 551 (1978)
25. A.V. Gurevich, R.G. Mints, Rev. Mod. Phys. **59**, 941 (1987)
26. A. Kiliç, K. Kiliç, O. Çetin, Physica C **384**, 321 (2003)
27. Z.L. Xiao, E.Y. Andrei, P. Ziemann, Phys. Rev. B **58**, 11 185 (1998)
28. D. Dimos, P. Chaudhari, J. Mannhart, Phys. Rev. B **41**, 4038 (1990)
29. H. Hilgenkamp, J. Mannhart, Rev. Mod. Phys. **74**, 485 (2002)
30. E.A. Gijsbertse, L.J.M. van de Klundert, M.L.D. van Rij, W.J. van Weezep Cryogenics **21**, 419 (1981)